

Stability of the fixed point of the two-channel Kondo Hamiltonian

H. B. Pang and D. L. Cox

Department of Physics, The Ohio State University, Columbus, Ohio 43210

(Received 3 May 1991)

We have performed full-scale numerical-renormalization-group calculations on the anisotropic, two-channel, impurity spin $s = \frac{1}{2}$ Kondo Hamiltonian. To allow for anisotropy we have worked in a basis of total axial charge j_a and j_b (a and b index the channels) as well as total S_z . In the isotropic limit, our results agree well with the previous work of Cragg, Lloyd, and Nozieres. The most important results are (1) confirmation of the approach to a nontrivial fixed point from weak coupling, (2) the stability of the fixed point against exchange anisotropy, and (3) the destabilization of the fixed point by the application of a magnetic field or the lifting of exchange symmetry between two channels. We find the crossover temperature scales with the square of the exchange splitting.

I. INTRODUCTION

The multichannel Kondo problem has been of interest since Nozieres and Blandin¹ showed that an anomalous fixed point occurs at finite coupling for $n > 2s$, where n is the channel number and s is the impurity spin. They also showed that this anomalous fixed point is unstable with respect to channel symmetry breaking and therefore suggested the unusual behavior at this fixed point could not be observed in real Kondo systems. Interest in the multichannel Kondo problem was renewed when Cox and co-workers²⁻⁴ proposed a quadrupolar Kondo Hamiltonian for uranium heavy-fermion materials and the cuprate high-temperature superconductors, which can be mapped exactly to a two-channel, pseudospin $s = \frac{1}{2}$ Kondo model. In Cox's model, the channel degeneracy is guaranteed by time reversal, but the exchange isotropy and pseudospin degeneracy are not guaranteed. It is therefore important to study the stability of the anomalous fixed point against anisotropy and the imposition of a magnetic field.

In this paper, we have performed numerical renormalization-group⁵ (NRG) calculations on the anisotropic two-channel, spin $s = \frac{1}{2}$ Kondo Hamiltonian. For the strong-coupling isotropic limit, our results agree well with the previous work of Cragg *et al.*⁶ For weak coupling J , as expected, the effective coupling flows to the anomalous fixed point after renormalization. The important new result is that the fixed point is stable against exchange anisotropy. We have also studied the fixed point when a magnetic field and channel-symmetry-breaking fields are applied to the impurity. We find that the anomalous fixed point is unstable in both cases.

In Sec. II, we will present the two-channel, spin $s = \frac{1}{2}$ Hamiltonian and its logarithmic discretized form. In Sec. III, we will discuss the symmetry of the Hamiltonian and methods we use. In Sec. IV, we will give the results for (1) bare J , which is small, (2) a bare Hamiltonian, which has exchange anisotropy, (3) a bare Hamiltonian with a magnetic field present, and (4) a bare Hamiltonian

with channel asymmetry induced via different exchange coupling.

II. HAMILTONIAN

The two-channel Kondo Hamiltonian is

$$H/D = \sum_k \epsilon_k c_{k\alpha\mu}^\dagger c_{k\alpha\mu} - \frac{1}{2} \sum_\alpha J_\alpha c_{0\alpha\mu}^\dagger \sigma_{\mu\nu} c_{0\alpha\nu} \cdot \mathbf{s} \quad (1)$$

Here D is the conduction bandwidth, $\alpha = a, b$, the index of two channels, μ is the spin index, $c_{k\alpha\mu}^\dagger$ are the usual electron creation operators, $c_{0\alpha\mu}^\dagger$ create electrons at the original site, σ is the vector of the Pauli matrices, and $s = \frac{1}{2}$ is the spin of impurity. Hamiltonian (1) will be logarithmically discretized in order to use the numerical renormalization-group method. For a more detailed discussion, see Sec. II of Ref. 7. Here is a brief outline of the method: (i) Divide the conduction band into logarithmic intervals, e.g., $\pm(\Lambda^{(n+1)} \text{ to } \Lambda^{-n})D$, with D the bandwidth and $\Lambda > 1$; (ii) keep only the average states in each interval (those are the ones that couple to the impurity); and (iii) for numerical convenience convert to a tridiagonal basis via the Lanczos algorithm with the initial state being the Wannier orbital about the impurity site. The Lanczos states correspond to creation operators $f_0^\dagger, f_1^\dagger, \dots$ and have a radial extent $\Lambda^{1/2}, \Lambda^{3/2}, \dots$ times k_{Fermi}^{-1} about the impurity. The final Hamiltonian has the form

$$H/D = \sum_{n=0}^{\infty} \epsilon_n (f_{n\alpha\mu}^\dagger f_{n+1\alpha\mu} + \text{H.c.}) - \sum_\alpha J_\alpha f_{0\alpha\mu}^\dagger \sigma_{\mu\nu} f_{0\alpha\nu} \cdot \mathbf{s}, \quad (2)$$

where

$$\epsilon_n = \frac{\Lambda^{-n/2}(1+\Lambda^{-1})(1-\Lambda^{-(n+1)})}{2[(1-\Lambda^{-(2n+1)})(1-\Lambda^{-(2n+3)})]^{1/2}}.$$

When $J_a = J_b$, one has the isotropic two channel Kondo Hamiltonian, while $J_a \neq J_b$ corresponds to the channel

asymmetric case. For the exchange anisotropic case, the term $J_a f_{0\alpha\mu}^\dagger \sigma_{\mu\nu} f_{0\alpha\nu}$'s is reduced by

$$J_a^\dagger f_{0\alpha\mu}^\dagger \sigma_{\mu\nu} f_{0\alpha\nu} S^z + \frac{1}{2} J_a^\dagger (f_{0\alpha\mu}^\dagger \sigma_{\mu\nu}^\dagger f_{0\alpha\nu} S^- + \text{H.c.}),$$

and $J_a^z = J_b^z$, $J_a^1 = J_b^1$, but $J_a^z \neq J_b^1$.

III. SYMMETRY

Now let us discuss the symmetry of the Hamiltonian (2). For the isotropic Hamiltonian, we make use of the conservation of the axial charges⁸ j_a, j_a^z, j_b, j_b^z , and of the total spin S, S^z . To allow for anisotropy, nondegeneracy, and a magnetic field, the remaining conserved quantities used in diagonalization are j_a, j_a^z, j_b, j_b^z , and S^z .

The axial charge and total S^z are defined as

$$\begin{aligned} j_a^+ &= \sum_{n=0}^{\infty} (-1)^n f_{n\alpha\uparrow}^\dagger f_{n\alpha\downarrow}^\dagger, \\ j_a^z &= \frac{1}{2} \sum_{n=0}^{\infty} (f_{n\alpha\uparrow}^\dagger f_{n\alpha\uparrow} + f_{n\alpha\downarrow}^\dagger f_{n\alpha\downarrow} - 1), \\ S^z &= \frac{1}{2} \sum_{\alpha,n=0}^{\infty} (f_{n\alpha\uparrow}^\dagger f_{n\alpha\uparrow} - f_{n\alpha\downarrow}^\dagger f_{n\alpha\downarrow}). \end{aligned} \quad (3)$$

The axial charge operators obey the same commutation relation as those of angular momentum, and j_a^2, j_a^z commute with the Hamiltonian. The good quantum numbers for the system are $|j_a j_a^z j_b j_b^z S^z\rangle$. We can diagonalize the Hamiltonian in each irreducible subspace $|j_a, j_b, S^z\rangle$. In our calculation, about 250 total states were retained at each iteration, and energies were measured in units of the conduction bandwidth.

IV. RESULTS

First we consider the isotropic, strong coupling limit. We have calculated the lowest energy levels for

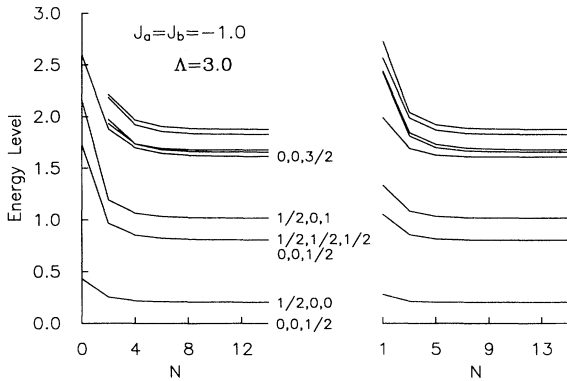


FIG. 1. Lowest numerical renormalization-group (NRG) energy levels for the strong-coupling isotropic two-channel Kondo Hamiltonian. We take the exchange couplings (J_a, J_b) of the channels to be equal to -1.0 , which is somewhat larger than the nontrivial fixed-point values. For all figures, energies are measured in units of the conduction bandwidth. For both even and odd iterations the levels flow quickly to the fixed point spectrum. The states here are labeled by the axial charges j_a, j_b and total spin S .

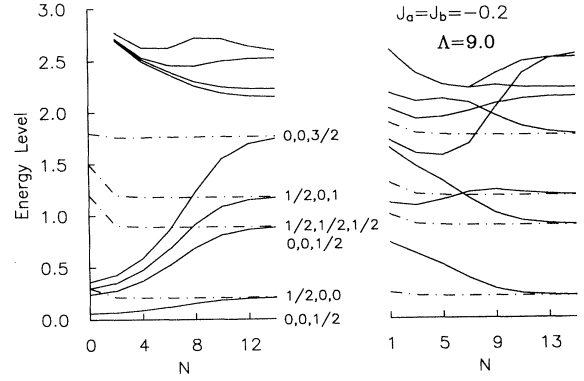


FIG. 2. Lowest NRG energy levels for the weak-coupling, isotropic two-channel Kondo Hamiltonian. We use $J_a = J_b = -0.2$ and choose the logarithmic discretization parameter $\Lambda = 9.0$ to ensure quick convergence. Although there are even-odd effects at the first few iterations, the energy spectrum eventually goes to a single fixed point when iteration N increases. By comparison, the dashed line represents the energy levels for the case $J_a = J_b = -1.0$ with the same $\Lambda = 9.0$. Differences in fixed point level spacings relative to Fig. 1 arise from the different choice of Λ .

$J_a = J_b = -1.0$, $\Lambda = 3.0$. The results shown in Fig. 1 agree well with the work of Cragg, Lloyd, and Nozieres.⁶ The energy spectrum goes to the fixed point after a few iterations, and there is no even-odd effect. In Fig. 2, we display the lowest-energy levels for weak coupling, with $J_a = J_b = -0.2$, $\Lambda = 9.0$ as a function of iteration number N . Because J is small, it takes many iterations for the spectrum to near the fixed point for $\Lambda = 3.0$. Large Λ value can greatly speed up convergence. In this figure, there is an odd-even effect up to the eighth iteration; after that the spectrum flows to the same fixed point as is reached starting with $J_a = J_b = -1.0$, $\Lambda = 9.0$.

Figure 3 gives the results for the exchange anisotropic

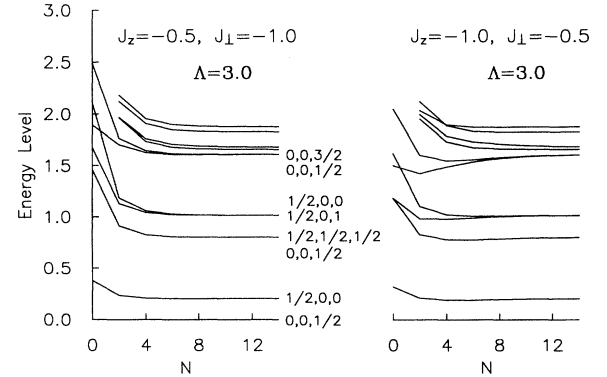


FIG. 3. Lowest NRG energy levels for the strong-coupling, two-channel Kondo model with exchange anisotropy. For both $J_z > J_\perp$ and $J_z < J_\perp$, the energy levels flow to the isotropic fixed point. The states here are labeled by j_a, j_b , and S_z .

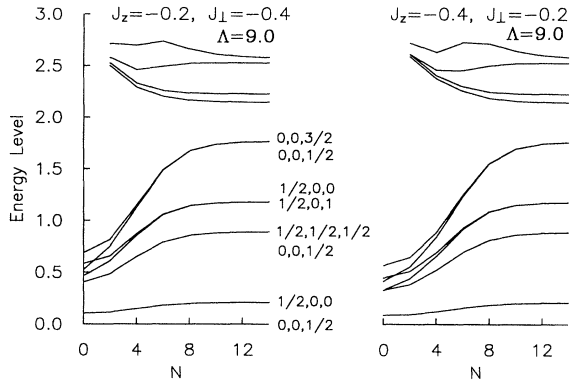


FIG. 4. Lowest NRG energy levels for the weak-coupling, two-channel Kondo model with exchange anisotropy. The energy levels flow to the isotropic fixed point. The states here are labeled by j_a , j_b , and S_z .

case with (a) $J^z = -0.5$, $J^\perp = -1.0$, and $\Lambda = 3.0$ and (b) $J^z = -1.0$, $J^\perp = -0.5$, and $\Lambda = 3.0$. The energy spectrum converges to the isotropic fixed point in both cases, indicating that the anomalous fixed point is stable with respect to exchange anisotropy. The same is true for the weak coupling case as is shown in Fig. 4.

Next we consider the effect of imposing a magnetic field, H . The fixed point for $J_a = J_b = -1.0$, $H = 0.12$, and $\Lambda = 3.0$ shown in Fig. 5, is a polarized Fermi-liquid fixed point. This means that the nontrivial fixed point is unstable when there is a magnetic field.

It was known^{1,6} prior to this work that the fixed point is unstable if $J_a \neq J_b$, and the system flows to the single-channel Kondo fixed point⁵ $J_{\min}^* = -\infty$, $J_{\max}^* = 0.0$. Our calculations confirm this result. From the calculation, the energy difference between the ground state ($|S_z| = \frac{1}{2}$) and first excited state ($|S_z| = 0$) is zero at the normal fixed point. This can be understood from the normal Kondo problem. In the one-channel Kondo problem, for the fixed point at $J = 0.0$, the first excited energy is zero for

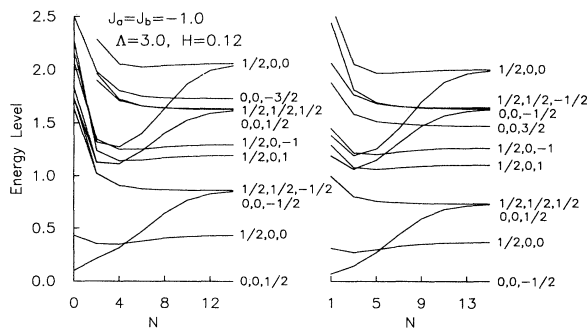


FIG. 5. Lowest NRG energy levels for the strong-coupling two-channel Kondo model in the presence of an applied magnetic field. The applied field destabilizes the nontrivial fixed point producing a flow to a polarized Fermi-liquid spectrum (to be discussed in a separate work). The quantum numbers here are j_a , j_b , and S_z .

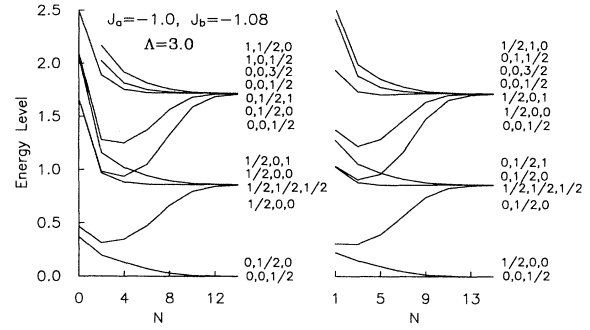


FIG. 6. Lowest NRG energy levels for the strong-coupling, two-channel Kondo model in a splitting of coupling for two channels. Lifting the channel degeneracy produces a flow to the normal Kondo fixed point. The quantum numbers here are j_a , j_b , and S_z .

even iterations and finite for odd iterations, but for the fixed point at $J = -\infty$, the first excited energy is zero for odd iterations and finite for even iterations. In the two-channel case, at this fixed point, the two channels are decoupled, and the first excited energy always zero no matter whether the iteration is even or odd (see Fig. 6).

Let us look at the crossover region between the anomalous and normal fixed point. We define the crossover temperature scale T_f by $T_f = \Lambda^{-N_f/2}$, where N_f is the iteration when the first excited energy becomes one tenth of that at anomalous fixed point. In Fig. 7, our results for $J_a = -1.0$, $J_b = J_a - \Delta J$ show that the temperature scale T_f is proportional to $(\Delta J)^2$. This is consistent with conformal field theory.¹⁰

V. SUMMARY

Using the NRG method, we have studied the fixed point of the two-channel, impurity spin $s = \frac{1}{2}$ Kondo problem. In the isotropic case, the energy spectrum flows to the nontrivial fixed point even for weak coupling. An

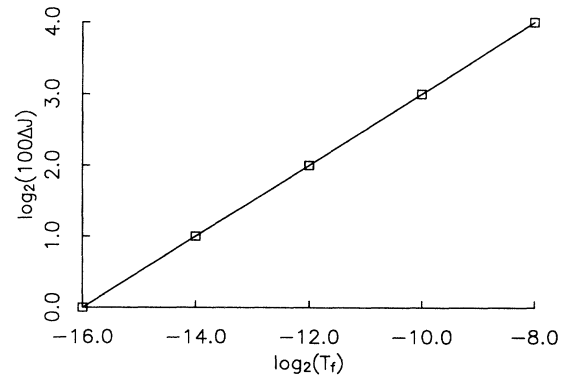


FIG. 7. Channel exchange splitting ΔJ vs crossover temperature scale T_f . T_f measures the temperature scale on which the energy levels crossover between the two fixed point (see text for definition). From this figure, we find that ΔJ is proportional to $T_f^{1/2}$.

applied field destabilizes the nontrivial fixed point. Interestingly, we find that the nontrivial fixed point is stable against the exchange anisotropy. We also find that the crossover temperature scale is proportional to $(\Delta J)^2$ when there is channel exchange splitting ΔJ . The comparison of our NRG results with the finite-size spectrum given by conformal field theory¹⁰ is planned to be discussed in another paper.

ACKNOWLEDGMENTS

We would like to thank I. Affleck, A. Ludwig, A. Tsvelik, B. A. Jones, C. M. Varma, and J. W. Wilkins. We would like to thank K. Ingersent for a careful reading of the manuscript. This work was supported by the Department of Energy, Office of Basic Energy Sciences, Division of Materials Research.

¹P. Nozieres and A. Blandin, *J. Phys. (Paris)* **41**, 193 (1980).

²D. L. Cox, *Phys. Rev. Lett.* **59**, 1240 (1987); *Physica C* **153-155**, 1642 (1988).

³D. L. Cox, M. Jarrell, C. Jayaprakash, H. R. Krishna-murthy, and J. Deisz, *Phys. Rev. Lett.* **62**, 2188 (1989); M. Jarrell and D. L. Cox, *Phys. Rev. B* **42**, 7690 (1990).

⁴D. L. Cox (unpublished).

⁵K. G. Wilson, *Rev. Mod. Phys.* **47**, 773 (1975).

⁶D. M. Cragg, P. Lloyd, and P. Nozieres, *J. Phys. C* **13**, 803

(1980).

⁷H. R. Krishna-murthy, J. W. Wilkins, and K. G. Wilson, *Phys. Rev. B* **21**, 1003 (1980).

⁸B. A. Jones, C. M. Varma, and J. W. Wilkins, *Phys. Rev. Lett.* **61**, 125 (1988).

⁹P. D. Sacramento and P. Schlottmann, *Phys. Rev. B* **43**, 13 294 (1991).

¹⁰I. Affleck and A. Ludwig, *Nucl. Phys. B* (to be published).